

Nucleation and Atomic Layer Reaction in Nickel Silicide for Defect-Engineered Si Nanochannels

Wei Tang,^{*,†,‡} S. Tom Picraux,[‡] Jian Yu Huang,[§] Andriy M. Gusak,^{||} King-Ning Tu,[†] and Shadi A. Dayeh^{*,‡,⊥}

[†]Department of Materials Science and Engineering, University of California, Los Angeles, Los Angeles, California 90024, United States

[‡]Center for Integrated Nanotechnologies, Los Alamos National Laboratory, Los Alamos, New Mexico 87545, United States

[§]Center for Integrated Nanotechnologies, Sandia National Laboratories, Albuquerque, New Mexico 87123, United States

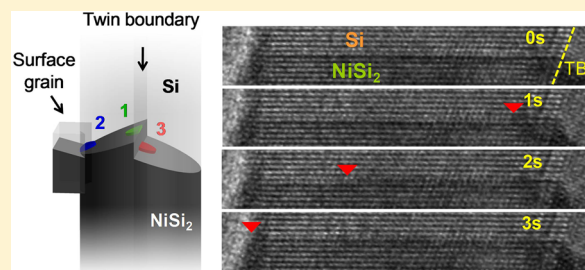
^{||}Department of Theoretical Physics, Cherkasy National University, Cherkasy, Ukraine

[⊥]Department of Electrical and Computer Engineering, University of California San Diego, La Jolla, California 92093, United States

Supporting Information

ABSTRACT: At the nanoscale, defects can significantly impact phase transformation processes and change materials properties. The material nickel silicide has been the industry standard electrical contact of silicon microelectronics for decades and is a rich platform for scientific innovation at the conjunction of materials and electronics. Its formation in nanoscale silicon devices that employ high levels of strain, intentional, and unintentional twins or grain boundaries can be dramatically different from the commonly conceived bulk processes. Here, using in situ high-resolution transmission electron microscopy (HRTEM), we capture single events during heterogeneous nucleation and atomic layer reaction of nickel silicide at various crystalline boundaries in Si nanochannels for the first time. We show through systematic experiments and analytical modeling that unlike other typical face-centered cubic materials such as copper or silicon the twin defects in NiSi₂ have high interfacial energies. We observe that these twin defects dramatically change the behavior of new phase nucleation and can have direct implications for ultrascaled devices that are prone to defects or may utilize them to improve device performance.

KEYWORDS: Nickel silicide, silicon nanowire, defects, twin boundary, heterogeneous nucleation, in situ TEM



Certain novel crystal growth phenomena are often attributed to nanocrystalline boundaries.^{1,2} These boundaries were found to significantly alter the electronic structure of semiconductor materials.^{3,4} An atomic level understanding of the silicidation process in the vicinity of such nanocrystallite boundaries can shed light on novel solid-state reactions at nanoscale and can bring their material⁵-electronic⁶ property interactions to new frontiers.⁷ In crystalline Si nanochannels (e.g., nanowires), nickel silicide grows by atomic layer reaction with repeating two-dimensional (2D) homogeneous nucleation and layer-by-layer growth.⁸ Heterogeneous nucleation is suppressed in this case because the only available heterogeneous site, the Si/native oxide interface is unfavorable owing to the need of creating a higher energy silicide-oxide interface. Therefore, the concentration of Ni atoms in the Si nanowire (NW) continues to soar until it reaches a level that is sufficient to initiate 2D homogeneous nucleation at the center of the Si/silicide interface in the Si NW. In nanostructures, this process can be dramatically different in the presence of crystallites and crystalline defects that introduce additional interfaces for nucleation, and such processes have not been studied before. Here, twin boundaries (TBs) and grain boundaries (GBs)

(often found in advanced semiconductor devices)^{9–13} are intentionally built into our Si NWs to specifically study the impact of these defects on nickel silicide nucleation and step flow in Si. By using in situ high-resolution transmission electron microscopy (HRTEM), the atomic layer silicidation reaction was monitored dynamically in real time to validate and examine the nature of nucleation and step flow at TB and surface GB heterogeneous nucleation sites. Our observation of different nucleation events near TBs and GBs are repeatable on more than five nanowire samples and is consistent with the data presented and analyzed below.

Our platform for the in situ TEM heating experiment was fabricated on a 50 nm thick electron-beam transparent silicon nitride TEM membrane where Ni metal contact formation to Si NWs predeposited onto such membranes has been described in detail elsewhere.¹⁴

To examine the influence of defects on silicide nucleation and growth, we first discuss the case of a Si NW with a twin

Received: March 14, 2013

Revised: May 19, 2013

Published: May 28, 2013

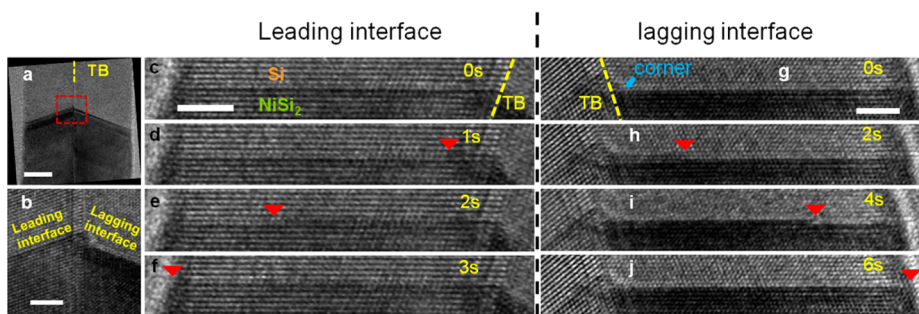


Figure 1. (a) Si NW with a TB, marked by the dashed yellow line, running down its central axis. Scale bar is 10 nm. (b) Zoom-in image of the red dashed box in panel (a) showing asynchronous growth of a leading interface and a lagging interface. Scale bar is 3 nm. (c–f) Nucleation and propagation of a (111) NiSi₂ plane at the leading interface from the TB. Scale bar is 3 nm. (g–j) Asynchronous nucleation from the corner interface between the silicided twin and unsilicided twin segment and propagation of a (111) NiSi₂ plane at the lagging interface. Scale bar is 3 nm.

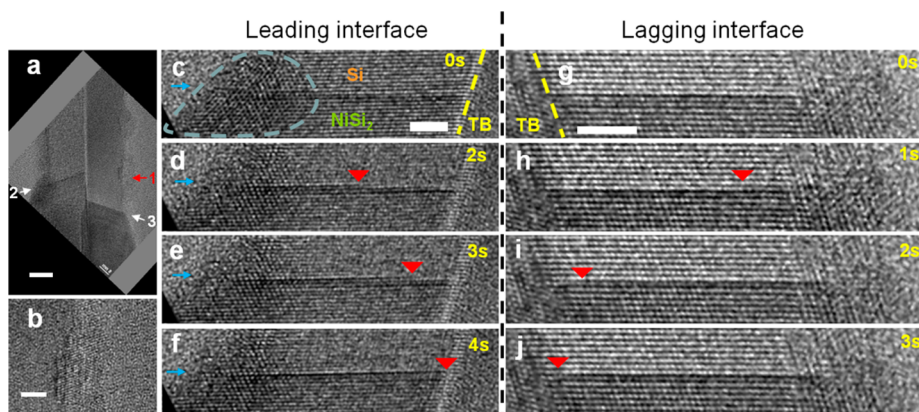


Figure 2. (a) Si NW with TB running along its central axis with GBs present at its surface. One example of a surface grain is indicated by “1”. The leading interface and another surface grain are indicated by “2” and the lagging interface is indicated by “3”. Scale bar is 10 nm. (b) Zoom-in HRTEM image of a cluster of surface grains (indicated by “1” in panel a) that have different crystallographic orientations with respect to the NW stem. Scale bar is 3 nm. (c–f) HRTEM snapshots (area indicated by “2” in panel a) of nucleation and propagation of a (111) NiSi₂ plane from the surface GB at the leading interface. The dashed light blue enclosure highlights the presence of a GB at the surface of the NW, and the blue arrow points at a reference mark on the NW edge. Scale bar is 3 nm. (g–j) Nucleation and propagation of a (111) NiSi₂ plane at the lagging interface (area indicated by “3”) from the surface GB. Scale bar is 3 nm.

defect running along its axis as shown in Figure 1a. The NW is essentially a bicrystal consisting of two portions of Si sharing a {111} plane, forming a coherent $\Sigma 3$ (111) twin boundary with NW axis along the (112) orientation.¹⁵ We find that the silicide growth front moves asynchronously in each of the bicrystals. We hereby refer to the fast growing interface as the leading interface and to the slower one as the lagging interface (Figure 1b). Figure 1c–f shows a series of in situ TEM snapshots providing direct evidence that a new NiSi₂ (111) plane nucleates at the TB (Figure 1c,d) and propagates on Si(111) plane at the leading interface and toward the edge surface of the NW (Figure 1e,f) in a layer-by-layer manner (see also Video 1 available in Supporting Information). Significantly, the new layer cannot directly propagate across the TB but rather remains in the same half of the twinned-bicrystal at which a nucleus was initially formed, and the new silicide nucleus does not form across the TB either. The formation of an individual nucleus on one side of the TB is energetically preferred as we will discuss below. As a consequence, the growth front of two halves of the bicrystal move asynchronously, and there is a chance to develop steps with heights of a few NiSi₂ (111) planes between the two interfaces. These observations show that step nucleation and flow on NiSi₂ in the presence of a twin boundary is dramatically different from that in a single crystal,⁸

where each new nickel silicide layer nucleates at the center of the nanowire in the reacting front.

Growth of NiSi₂ (111) plane at the lagging interface also proceeds in a layer-by-layer manner (Supporting Information Video 1). A new NiSi₂ (111) plane nucleates at the “corner” (marked in Figure 1g) and then propagates to the edge surface of the NW (Figure 1g–j). The nucleation at the lagging interface is expected to be more energetically favorable when compared to the leading interface because it annihilates part of the high energy NiSi₂/Si interface. These distinct observations on the formation of a new phase nucleus and step flow are the first to be captured in real time at crystalline boundaries and confirm unambiguously the location of the nucleus at the TB.

In addition to TBs, Si grains can also form in the processing of nanoscale semiconductor devices.^{12,13} It is therefore interesting to investigate the influence of grain boundaries at the nanowire surface on silicide nucleation. We find that heterogeneous nucleation is further facilitated at surface grain boundaries. Figure 2a shows a twinned Si NW with surface grains, and Figure 2b highlights several surface grains with different crystallographic orientations with respect to the stem of the NW. In situ TEM snapshots in Figure 2c–f show at the leading interface a single NiSi₂ layer first nucleates at the surface GB and propagates toward the center of the NW (see also

Video 2 in Supporting Information). Here, the surface grain partially overlaps with the NW along the viewing direction (marked by light blue dashed enclosure). The NiSi₂ (111) step flow is opposite in direction to the case where no surface GBs are present on the NW (e.g., Figure 1c–f). We note that this is due to a much higher GB energy than TB energy and quantitative analysis of this effect will be shown next. In the presence of a GB at the nanowire surface, the NiSi₂ growth also proceeds into the surface GB.

In contrast to the situation in Figure 1g–j, at the lagging interface of a Si NW with both TBs and GBs (Figure 2g–j) we see that the presence of the surface GB can pin the nucleation site at the surface GB instead of the corner region at the center of the TB. Figure 2g–j shows one example in which the new NiSi₂ (111) plane nucleates from surface GB and then propagates toward the center of the NW (see also Video 3 in Supporting Information). It is tempting to infer that a NiSi₂ twin has a low energy, because NiSi₂ has a face-centered cubic (fcc) structure, which is similar to Cu and Si, and the latter two have a much lower TB energy than the GB energy or heterointerface energy.^{16,17} The formation of a coherent TB of Cu or Si only involves alternation of the stacking sequence and the nearest neighbor coordination of interfacial atoms is not disturbed. If the NiSi₂ twin does have a low energy, nucleation at the “corner” should be very fast. However, a close look at the structure of the TB in a NiSi₂ crystal reveals that the nearest neighbor configurations of the interfacial atoms are in fact disturbed (Supporting Information Figure S1) and are no longer the same as those in the bulk, so the TB energy in NiSi₂ is not negligible, as calculated in the Supporting Information. This also explains why NiSi₂ (111) planes do not nucleate or propagate across the TB as was demonstrated in Figure 1c–f, since nucleation at the “corner” would not be favored because of the need to create a high-energy NiSi₂ TB.

To quantitatively assess the layer-by-layer growth of NiSi₂ in the presence of crystalline defects, we tracked over an extended period of time the NiSi₂ (111) plane nucleation and step migration. The in situ experiment provides for the precise measurement of growth rate behavior of NiSi₂ in Si NWs. We observe a distinctive behavior in nucleation and step migration when assisted by TB alone (Figure 3a) versus by GB when the TB/GB coexist in the same NW (Figure 3b). In Figure 3a, the growth (in both halves of Si bicrystal) is almost linear over a time period exceeding 20 min featuring a steady growth rate. Note that the growth was monitored when the silicide segment extending from the reference Ni electrode grows from 547 to 586 nm. The growth rate does not significantly change during this period of time because the Ni diffusion length (silicide segment length) is relatively unchanged. Therefore, the linear growth observed here does not conflict with previously reported^{18,19} parabolic growth behavior. The blue curves in Figure 3 indicate the height difference (referred to asynchronous step height, or ASH, hereafter) between the silicide/silicon interface in each half of the bicrystal, that is, leading and lagging interfaces. ASH of several (111) planes can develop because the nucleation of a new plane at leading or lagging interfaces represents independent random events. However, the lagging interface can catch up with the leading interface because the corner is a more preferable heteronucleation site, so on the average ASH does not grow significantly, given that Ni supply is equally available for both halves of the bicrystal. On the other hand, when surface GBs are further introduced onto the NW, the growth rate fluctuates and can change by a factor of 3.8

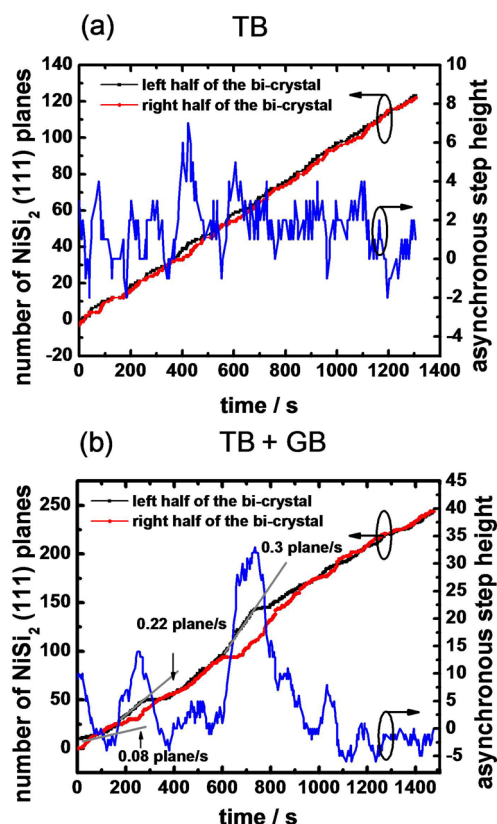


Figure 3. Growth of NiSi₂ (111) plane and asynchronous step height (see text) evolution in Si NW with (a) TB and (b) both TB and GB. The NiSi₂ (111) plane spacing is 0.31 nm. Within the period of observation, a single TB maintains a steady linear growth rate in (a) whereas the high energy of the surface GB promotes intermittent fast growth with periods superposed on a linear trend in (b).

(from 0.08 plane/s to 0.3 plane/s) over a similar NiSi₂ growth time.

The irregular growth behavior in the presence of surface GBs originates from the fact that the nucleation barrier of each new NiSi₂ (111) plane depends on the energy of surface GBs, which is a function of relative orientation of the surface grain with respect to the NW as well as the details of the atom arrangements at the GB. On the segment of the NW with high energy surface GBs, heterogeneous nucleation is more favored and the NiSi₂ grows faster. We note that in the time period between 600 and 630 s in Figure 3b the leading interface (black curve, left portion in the bicrystal) grows rapidly, while the growth of the lagging interface (red curve, right portion in the bicrystal) ceases, and a huge ASH (with a maximum height of 33 NiSi₂ (111) atomic layers) develops as a result between these two interfaces. Rapid growth of the leading interface implies high GB energy at the surface, which promptly assists nucleation of NiSi₂ and consume incoming Ni atoms to complete the layer-by-layer growth. Therefore, the NiSi₂ nuclei preferably formed at the leading interface GB act as Ni sinks and keep the Ni concentration at the lagging interface lower than that required to nucleate a new NiSi₂ plane. In this extreme case, NiSi₂ growth is completely dominated by nucleation at extrinsic surface GBs and shadows other intrinsic nucleation sites like the corner so that the lagging interface does not grow for an extended period of time. This result suggests that the defects can play a prominent role in the nickel silicide formation process. To use silicide as S/D extensions in

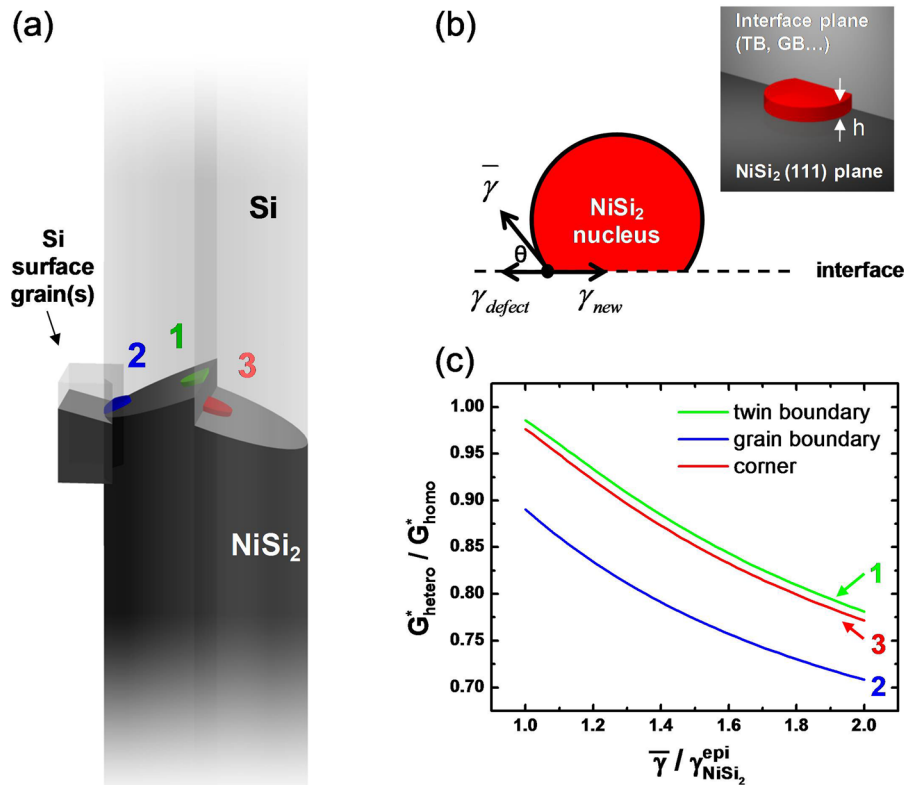


Figure 4. (a) Schematic of three different heterogeneous nucleation sites. (b) Top view of a NiSi₂ 2D partial disk heterogeneously nucleated at a certain interface with an inset of its arrangement in 3D. (c) Reduction in the nucleation barrier at different heterogeneous sites.

nanoscale Si-based devices, controlled growth of nickel silicide into 3D Si channels is extremely important and since device-to-device variation is undesirable such surface defects must be avoided.

Our experimental observations can be validated by an intuitive quantitative model based on classical nucleation theory by considering different types of defects. We consider the following heterogeneous sites: (1) Si TB, (2) Si GB, and (3) the TB corner, as depicted in Figure 4a, and discuss the corresponding interface energy parameters separately. For a silicide nucleus (Figure 4b) and assuming the 2D silicide partial disk nucleates at a certain interface in the system, the total change in the system free energy, ΔG_{hetero} , is given by

$$\Delta G_{\text{hetero}} = -\Delta g \left[\pi R^2 \left(\frac{1-\theta}{\pi} \right) + R^2 \sin(\theta)\cos(\theta) \right] h + 2(\pi - \theta)Rh\bar{\gamma} + 2Rh \sin(\theta)(\gamma_{\text{new}} - \gamma_{\text{defect}}) \quad (1)$$

where Δg is the silicide formation energy, R is the radius of the disk, h is the height of one atomic step, θ is the contact angle, $\bar{\gamma}$ is the average interface energy between NiSi₂ and Si over different orientations, γ_{defect} is the original defect energy, γ_{new} is the energy of the interface subject to nucleation with NiSi₂ at the original defect boundary. Both γ_{defect} and γ_{new} assumes different values for different defects which will become clear as we discuss specific defect types below.

The critical radius, R^* , can be solved by letting $\partial\Delta G/\partial R|_{R=R^*} = 0$, and invoking the Young's equation ($\bar{\gamma} \cos(\theta) + \gamma_{\text{defect}} = \gamma_{\text{new}}$) to result in the heterogeneous nucleation energy barrier

$$\Delta G_{\text{hetero}}^* = \frac{\bar{\gamma}^2 h}{\Delta g} [(\pi - \theta) + \sin(\theta)\cos(\theta)] \quad (2)$$

For the special case of $\theta = 0$, eq 2 gives the homogeneous nucleation barrier $\Delta G_{\text{hetero}}^* = (\pi\bar{\gamma}^2 h)/(\Delta g)$. To determine the impact of defects on reducing the nucleation energy barrier, we calculate the ratio

$$\frac{\Delta G_{\text{hetero}}^*}{\Delta G_{\text{homo}}^*} = \frac{(\pi - \theta) + \sin(\theta)\cos(\theta)}{\pi} \quad (3)$$

The exact choice of interface energy parameters is discussed in detail in the Supporting Information. Table 1 provides a

Table 1. Summary of Interfacial Energy Parameters Used in the Nucleation Model for All Three Cases Considered in Figure 4

nucleation boundary type	γ_{defect}	γ_{new}
TB	$\gamma_{\text{Si}}^{\text{twin}}$ (0.05 J/m ²)	$\gamma_{\text{Si-NiSi}_2}^{\text{epi}}$ (0.6 J/m ²)
GB	$\gamma_{\text{Si}}^{\text{GB}}$ (0.4 J/m ²)	$\gamma_{\text{Si-NiSi}_2}^{\text{inc}}$ (0.8 J/m ²)
NiSi ₂ /Si twinned interface	$\gamma_{\text{Si-NiSi}_2}^{\text{epi}}$ (0.6 J/m ²)	$\gamma_{\text{NiSi}_2}^{\text{twin}}$ (1.13 J/m ²)

summary of the interfacial energetic parameter values. The TB energy in NiSi₂, $\gamma_{\text{NiSi}_2}^{\text{twin}}$ is not known from the literature. We developed a stochastic mathematical model to depict the asynchronous silicide growth process in a twinned Si NW as a biased 1D random walk in the ASH space. We derive the statistical average ASH from the model and relate it to the experimental measured value (average of blue curves in Figure 3a) to extract $\gamma_{\text{NiSi}_2}^{\text{twin}} = 1.13 \text{ J/m}^2$. Details of the model are

described in the Supporting Information. This result demonstrates that unlike typical fcc materials (e.g., Si, Cu, etc.) with typical energies 20–50 mJ/m²,^{16,17} the TB defect in NiSi₂ has a high interfacial energy, which is determined by the detailed atomic arrangement in its unit cell.

Figure 4c shows the effectiveness of nucleation barrier energy reduction $\Delta G_{\text{hetero}}^*/\Delta G_{\text{homo}}^*$ by nucleation at various types of defects or heterogeneous sites. The ratio $\bar{\gamma}/\gamma_{\text{Si/NiSi}_2}^{\text{epi}}$ accounts for the uncertainty of $\bar{\gamma}$ ($\gamma_{\text{Si/NiSi}_2}^{\text{epi}}$ or the energy of epitaxial Si/NiSi₂ interface, provides a reference) and is assumed over a certain range as shown in Figure 4c. As a conservative estimate, we choose $\Delta G_{\text{hetero}}^*/\Delta G_{\text{homo}}^*$ values to be 0.934, 0.924, and 0.835, for the nucleation at TBs, corners, and the GBs, respectively. In addition, we have computed $\Delta G_{\text{hetero}}^*/\Delta G_{\text{homo}}^*$ for a range of $\gamma_{\text{NiSi}_2}^{\text{twin}}$ (see Figure S4 of the Supporting Information), and the results corroborate with those presented in Figure 4. Note that the nucleation rate is proportional to $\exp(-\Delta G^*/kT)$, so a slight change in the nucleation energy barrier can change the nucleation rate dramatically. The analysis here shows that defects can indeed change the nucleation behavior of the new silicide layer and various defects can be further differentiated by the amount of interfacial energy reduction after silicide nucleation.

There are two contributions to the heterogeneous nucleation energy barrier reduction, (i) formation of a low energy Si/NiSi₂ interface at the defect plane and (ii) annihilation of the defect itself. For heterogeneous nucleation at the TB, NiSi₂ nucleus can form a low energy epitaxial interface with Si, which facilitates heterogeneous nucleation. For nucleation at a Si GB, the reduction in nucleation energy is mainly provided by annihilation of the Si GB. Thus contribution (ii) plays an important role here and the nucleation energy barrier is even lower than the nucleation at Si TB. A general criterion for heterogeneous nucleation is that $\gamma_{\text{new}} - \gamma_{\text{defect}} < \bar{\gamma}$, which captures both contributions.

Although our studies focus on the Ni silicidation reaction in a NW system, they have general implications to the kinetics of contact formation and device reliability in very large scale integration (VLSI) technologies. In a CMOS fabrication process, the S/D region of MOSFETs needs to be heavily doped to achieve low contact resistances. This is typically accomplished by dopant implantation and subsequent S/D activation thermal anneal to recrystallize the damaged S/D area where defects may form during the annealing step. Yamaguchi et al.¹¹ found that Si(111) stacking faults form at the trench edge after S/D activation annealing, and that NiSi₂ whiskers form and elongate from such trench edges and pierce into the channel. The origin of this observation can be explained by the current study on enhanced heterogeneous nucleation of the NiSi₂ phase at stacking fault defects. While these stacking faults were unintentionally formed, as previously discussed, some are intentionally introduced in the S/D region to engineer tensile strain in n-type transistor channels and enhance electron mobilities through the strain memorization technology.^{9,10} Our studies imply that the presence of defects in the S/D region may change the contact silicidation process and undesired silicide encroachment into the channel may occur when silicide formation is guided by such defects. Our in situ TEM studies provide new insights into how nickel silicide formation interacts with various defect types in Si and can further guide defect engineering strategies to beneficially impact contact formation in VLSI device technologies.

Experimental Methods. Si NWs were grown by LPCVD as detailed before.²⁰ Post growth, the Si NWs were released from the substrate into isopropanol solution by ultrasound agitation in a water bath and were randomly dispersed on the silicon nitride membrane. Chess board patterns with alternative contact pad openings were defined by photolithography. The native oxide on the Si NW at the contact areas was completely removed by dipping in diluted buffered oxide etch (BOE) solution (6 parts 40% NH₄F and 1 part 49% HF) for 20 s. Deposition of a Ni film of 100 nm by electron-beam evaporation followed.

We use an in situ TEM heating stage (Gatan single tilt heating stage 628) to anneal the specimen in a TEM (FEI Tecnai 300 keV) chamber at a vacuum level of 10⁻⁸ Torr. The temperature is controlled by an external current source, and it allows isothermal heat treatment of the sample after the initial temperature transient (about 2 min). All samples discussed in this Letter were annealed at 300 °C. High-resolution (HR) TEM images are continuously updated by the CCD scan system, and frames were captured and compiled into videos to reveal the dynamic process of the silicide growth.

■ ASSOCIATED CONTENT

§ Supporting Information

Details on structure analysis of possible NiSi₂ twin structure, interface energy parameter selection, and stochastic 1D biased random walk model. This material is available free of charge via the Internet at <http://pubs.acs.org>.

■ AUTHOR INFORMATION

Corresponding Author

*E-mail: (W.T.) weitang@ucla.edu; (S.A.D.) sdayeh@ece.ucsd.edu

Notes

The authors declare no competing financial interest.

■ ACKNOWLEDGMENTS

This work was performed in part at the Center for Integrated Nanotechnologies (Proposal No. C2011A1023), a U.S. Department of Energy, Office of Basic Energy Sciences user facility. Los Alamos National Laboratory, an affirmative action equal opportunity employer, is operated by Los Alamos National Security, LLC, for the National Nuclear Security Administration of the U.S. Department of Energy under contract DE-AC52-06NA25396. We thank Professor Ning Wang from Hong Kong University of Science and Technology for training W.T. in TEM imaging. We thank Blythe Clark from Sandia National Laboratory for providing the in situ TEM heating stage and John Nogan for assistance in fabrication facilities at CINT. S.A.D. acknowledges support from a faculty start-up grant at the University of California San Diego.

■ REFERENCES

- (1) Frank, F. C. The influence of dislocations on crystal growth. *Discuss. Faraday Soc.* **1949**, *5*, 48.
- (2) Jin, S.; Bierman, M. J.; Morin, S. A. A New Twist on Nanowire Formation: Screw-Dislocation-Driven Growth of Nanowires and Nanotubes. *J. Phys. Chem. Lett.* **2010**, *1*, 1472.
- (3) Ahn, K. H.; Lookman, T.; Saxena, A.; Bishop, A. R. Electronic properties of structural twin and antiphase boundaries in materials with strong electron-lattice couplings. *Phys. Rev. B* **2005**, *71*, 212102.
- (4) Dayeh, S. A.; Susac, D.; Kavanagh, K. L.; Yu, E. T.; Wang, D. Structural and Room-Temperature Transport Properties of Zinc

Blende and Wurtzite InAs Nanowires. *Adv. Funct. Mater.* **2009**, *19*, 2102.

(5) Gosele, U.; Tu, K. N. Growth kinetics of planar binary diffusion couples: "Thin-film case" versus "bulk cases". *J. Appl. Phys.* **1982**, *53*, 3252.

(6) Tung, R. T. Schottky-Barrier Formation at Single-Crystal Metal-Semiconductor Interfaces. *Phys. Rev. Lett.* **1984**, *52*, 461.

(7) Wu, Y.; Xiang, J.; Yang, C.; Lu, W.; Lieber, C. M. Single-crystal metallic nanowires and metal/semiconductor nanowire heterostructures. *Nature* **2004**, *430*, 61.

(8) Chou, Y.-C.; Wu, W.-W.; Chen, L.-J.; Tu, K.-N. Homogeneous Nucleation of Epitaxial CoSi₂ and NiSi in Si Nanowires. *Nano Lett.* **2009**, *9*, 2337.

(9) Weber, C. E.; Cea, S. M.; Deshpande, H.; Golonzka, O.; Liu, M. Y. Modeling of NMOS performance gains from edge dislocation stress. *IEEE Int. Electron Devices Mtg.* **2011**, 34.4.1.

(10) Kwan-Yong, L.; Hyunjung, L.; Choongryul, R.; Kang-Ill, S.; Uihui, K.; Seokhoon, K. Novel stress-memorization-technology (SMT) for high electron mobility enhancement of gate last high-k/metal gate devices. *IEEE Int. Electron Devices Mtg.* **2010**, 10.1.1.

(11) Yamaguchi, T.; Kashihara, K.; Kudo, S.; Tsutsumi, T.; Okudaira, T.; Maekawa, K.; et al. Characterizations of NiSi₂-Whisker Defects in n-Channel Metal-Oxide-Semiconductor Field-Effect Transistors with $\langle 110 \rangle$ Channel on Si(100). *Jpn. J. Appl. Phys.* **2010**, *49*, 126503.

(12) Duffy, R.; Dal, M. J. H. V.; Pawlak, B. J.; Kaiser, M.; Weemaes, R. G. R.; Degroote, B.; et al. Solid phase epitaxy versus random nucleation and growth in sub-20 nm wide fin field-effect transistors. *Appl. Phys. Lett.* **2007**, *90*, 241912.

(13) Jeng-Tzong, S.; Po-Chun, H.; Tzu-Shiun, S.; Chen-Chia, C.; Lu-An, C. Characteristics of Gate-All-Around Twin Poly-Si Nanowire Thin-Film Transistors. *IEEE Electron Device Lett.* **2009**, *30*, 139.

(14) Tang, W.; Dayeh, S. A.; Picraux, S. T.; Huang, J. Y.; Tu, K.-N. Ultrashort Channel Silicon Nanowire Transistors with Nickel Silicide Source/Drain Contacts. *Nano Lett.* **2012**, *12*, 3979.

(15) Dayeh, S. A.; Wang, J.; Li, N.; Huang, J. Y.; Gin, A. V.; Picraux, S. T. Growth, Defect Formation, and Morphology Control of Germanium-Silicon Semiconductor Nanowire Heterostructures. *Nano Lett.* **2011**, *11*, 4200.

(16) Cockayne, D. J. H.; Jenkins, M. L.; Ray, I. L. F. The measurement of stacking-fault energies of pure face-centred cubic metals. *Philos. Mag.* **1971**, *24*, 1383.

(17) Mattheiss, L. F.; Patel, J. R. Electronic stacking-fault states in silicon. *Phys. Rev. B* **1981**, *23*, 5384.

(18) Chen, Y.; Lin, Y.-C.; Huang, C.-W.; Wang, C.-W.; Chen, L.-J.; Wu, W.-W.; et al. Kinetic Competition Model and Size-Dependent Phase Selection in 1D Nanostructures. *Nano Lett.* **2012**, *12*, 3115.

(19) Dellas, N. S.; Abraham, M.; Minassian, S.; Kendrick, C.; Mohny, S. E. Kinetics of reactions of Ni contact pads with Si nanowires. *J. Mater. Res.* **2011**, *26*, 2282.

(20) Picraux, S. T.; Dayeh, S. A.; Manandhar, P.; Perea, D.; Choi, S. Silicon and germanium nanowires: Growth, properties, and integration. *JOM* **2010**, *62*, 35.